AN EXTRAPOLATIVE APPROACH TO INTEGRATION OVER HYPERSURFACES IN THE LEVEL SET FRAMEWORK

CATHERINE KUBLIK AND RICHARD TSAI

ABSTRACT. We provide a new approach for computing integrals over hypersurfaces in the level set framework. The method is based on the discretization (via simple Riemann sums) of the classical formulation used in the level set framework, with the choice of specific kernels supported on a tubular neighborhood around the interface to approximate the Dirac delta function. The novelty lies in the choice of kernels, specifically its number of vanishing moments, which enables accurate computations of integrals over a class of closed, continuous, piecewise smooth, curves or surfaces; e.g., curves in two dimensions that contain a finite number of corners. We prove that for smooth interfaces, if the kernel has enough vanishing moments (related to the dimension of the embedding space), the analytical integral formulation coincides exactly with the integral one wishes to calculate. For curves with corners and cusps, the formulation is not exact but we provide an analytical result relating the severity of the corner or cusp with the width of the tubular neighborhood. We show numerical examples demonstrating the capability of the approach, especially for integrating over piecewise smooth interfaces and for computing integrals where the integrand is only Lipschitz continuous or has an integrable singularity.

1. INTRODUCTION

We propose an extrapolative approach for computing integrals over a class of piecewise smooth hypersurfaces, given implicitly via a level set function. The method is based on the classical approximation used in the level set framework that smears out the Dirac δ function to a bump function with a compact support. We analyze a family of integrals over the level sets of a Lipschitz continuous function whose zero level set defines the hypersurface, and use special kernels with vanishing moments for the approximation of the Dirac δ function. *The novelty is in how we combine the classical formulas for the more challenging cases in which the hypersurfaces have kinks and corners.* In particular, the proposed method does not require any local explicit parameterization of the hypersurface, nor the explicit locations of the corners and kinks on the hypersurface. The key to our results is the smoothness of this family of integrals with respect to the parameter η which is the signed distance between the zero level set Γ_0 and the "parallel" level set Γ_η.

We derive an estimate of the error in terms of the severity of the corner/cusp and the width of the kernels. This work lays the foundation of a numerical scheme for computing general improper integrals.

Let Γ_0 be a closed hypersurface in $\mathbb{R}^n$ (namely, a closed curve in $\mathbb{R}^2$ or closed surface in $\mathbb{R}^3$) defined implicitly as the zero level set of a level set function ϕ, namely

$$\Gamma_0 := \{\mathbf{x} : \phi(\mathbf{x}) = 0\}.$$

We are interested in computing integrals of the form

$$(1) \qquad\qquad I_0 := \int_{\Gamma_0} f(\mathbf{x}) dS(\mathbf{x}),$$

which is classically approximated in the level set framework [14] by

$$(2) \qquad\qquad S := \int_{\mathbb{R}^n} \tilde{f}(\mathbf{x}) \delta_\epsilon(\phi(\mathbf{x})) |\nabla \phi(\mathbf{x})| d\mathbf{x},$$

where $\tilde{f} : \mathbb{R}^n \to \mathbb{R}$ is Lipschitz constant along the normal of Γ_0 and $\tilde{f} = f$ on Γ_0.

We consider S as an average of a one-parameter family of integrals in η,

$$S = \int_{\mathbb{R}^n} \tilde{f}(\mathbf{x}) \delta_\epsilon(\phi(\mathbf{x})) |\nabla \phi(\mathbf{x})| d\mathbf{x} = \int_{-\epsilon}^{\epsilon} \delta_\epsilon(\eta) \left(\int_{\Gamma_\eta} \tilde{f}(\mathbf{x}) dS(\mathbf{x}) \right) d\eta$$

and *exploit the smoothness of this family of integrals with respect to η via suitable moment conditions on the kernel δ_ϵ.* Our first result shows that for smooth hypersurfaces in $\mathbb{R}^n$, S yields the exact value of I_0 if the kernel δ_ϵ has $n - 1$ vanishing moments. In our second result $\Gamma_0 \subset \mathbb{R}^2$ has a corner or a pth cusp singularity. The result states that if δ_ϵ has m vanishing moments and $\delta_\epsilon(\eta) = O(\epsilon^{-k})$, then for small $\epsilon > 0$,

$$|S - I_0| = \begin{cases} O\left(\epsilon^{2+m-k}\right) & p = 1 \text{ (corner)}, \\ O\left(\epsilon^{1+\frac{1}{p}-k}\right) & p \geq 2 \text{ (cusp)}. \end{cases}$$

This paper relates the geometry of the hypersurface and the smoothness of its corners to the choice of kernels needed to obtain a highly accurate numerical scheme for computing integrals over that hypersurface.

2. Motivation for the present work

2.1. **Background and related work.** This paper provides a new understanding of surface integrals in the level set framework, particularly in the case where the curve or surface Γ_0 is only piecewise smooth. It is of interest to study the integration over these types of hypersurfaces in the context of level set methods since there are many applications of level set methods in which the hypersurfaces go through topological changes in a dynamical process. In computer vision, for example, the segmentation of an image may be obtained via a two-dimensional flow using level set methods, in which case the flow will give rise to a curve undergoing topological changes and developing corners during its evolution. Level set methods have also been used in constrained optimization problems [10, 13], where the Lagrange multipliers can be expressed in terms of boundary integrals. In addition, boundary integral methods used in combination with level sets [2, 7, 8] have recently shown promising results. Other applications of implicit boundary integral methods include the computation of the Dirichlet-to-Neumann map in the context of shape optimization and the integration over streamlines in fluid mechanics. In this paper,

we shed light on a mathematical framework for integrating over piecewise smooth hypersurfaces defined implicitly via a level set function.

We focus on the situation where the information about Γ_0 is given only via the values of a level set function ϕ on some grid. We shall refer to the corresponding grid function by $\phi_{\mathbf{i}}$. There are two strategies for computing integrals like (1) in the level set framework:

(1) Derive local explicit approximations of the implicit surface, then derive quadrature rule based on the explicit, approximate surfaces. From the level set grid function $\phi_{\mathbf{i}}$, one typically approximates the curve or surface Γ_0 by $\Gamma_\triangle$, (generally a polygon), and then uses this approximation to compute the integral of f over Γ_0 using local parameterizations of $\Gamma_\triangle$ (see, e.g., [9, 18, 21]). Recently in [17]), it is proposed to convert the implicit geometry into the graph of an implicitly given height function, leading to a recursive algorithm on the number of dimensions and thus requiring only one-dimensional root-finding and one-dimensional Gaussian quadratures. The moment-fitting method from [11] requires special divergence-free bases and integration by parts.

(2) Derive an analytical integral formulation $I(f, \phi)$ that is *easy* to discretize, then discretize it (see, e.g., [7, 8, 21, 22, 25–28]). We note that this approach computes the integral (1) *without using any local parameterizations of* Γ_0.

In this paper, we consider the second approach. In the level set framework, the integral (1) is formally written in the form

$$(3) \qquad \int_{\mathbb{R}^n} f(\mathbf{x}) \delta(\phi(\mathbf{x})) |\nabla \phi| d\mathbf{x},$$

where $\delta(\cdot)$ denotes the Dirac delta function. Formula (3) is then approximated by (2), in which δ_ϵ is a bump (kernel) function that integrates to 1. The integral (2) over $\mathbb{R}^n$ is then discretized via simple Riemann sums on a Cartesian grid using a specific choice for $\delta(\cdot)$. There are many approximations or regularizations of $\delta(\cdot)$ in the numerical literature. Typically the regularized δ-function is defined on a tubular neighborhood around the interface of width ϵ, denoted δ_ϵ. This effectively thickens or diffuses the interface in that tubular neighborhood. One choice is to take ϵ independent of the level set function ϕ and the grid. In the work of Smereka [21], the discrete delta function is concentrated within one grid cell on either side of the interface, and is obtained by discretizing the fundamental solution of the Laplace equation using ghost-points. In the work of Towers [22], the discretized delta function is computed via two different formulations involving the Heaviside function. The more accurate formulation is obtained using integration by parts on a suitable integral. In [6], the Dirac delta function is regularized using the gradient of the level set function ϕ, a scaling that allows ϵ (the width of the tubular neighborhood around the interface) to be small with respect to the underlying grid. In the work of Burger et al. [1] the integration over a sufficiently smooth closed surface is approximated by an integral like (3) over a narrow band around the surface. The authors provide a detailed analysis of the convergence of the integral over the diffuse surface towards the integral over the surface. In particular, they provide different convergence rates depending on the smoothness of the integrand.

The framework for the present work started with [7] and [8] where the authors proposed and studied an integral formulation over the ambient space that coincides exactly with the line or surface integral that one wishes to calculate. This formulation is designed for curves and surfaces that are not defined by any explicit parameterizations and is intended to be used with level set techniques [12,20] or the closest point methods, e.g., [16]. In [8] the formulation is provided in dimensions two and three and extended to open curves and surfaces.

The integral formulation proposed in [7] and [8] allows the computation of integrals of the form (1), where Γ_0 is the zero level set of the signed distance function d to Γ_0, namely $\Gamma_0 := \{\mathbf{x} : d(\mathbf{x}) = \mathbf{0}\}$. The integral formulation is given by

$$(4) \qquad I_0 \equiv \int_{\mathbb{R}^n} f(P_{\Gamma_0}(\mathbf{x}))\delta_\epsilon(d(\mathbf{x}))J(\mathbf{x}; d(\mathbf{x}))d\mathbf{x},$$

where $P_{\Gamma_0} : \mathbb{R}^n \mapsto \Gamma_0$ is the closest point mapping to Γ_0 (or projection operator onto Γ_0) defined as

$$(5) \qquad P_{\Gamma_0}(\mathbf{x}) = \mathbf{x} - d(\mathbf{x})\nabla d(\mathbf{x}),$$

δ_ϵ is an averaging kernel specifying a tubular neighborhood around Γ_0, and $J(\mathbf{x}; d(\mathbf{x}))$ is the Jacobian that accounts for the change in curvature between nearby level sets and the zero level set Γ_0. The main advantage of formulation (4) is that unlike (3) which is an *approximation* of I_0 using a regularized Dirac δ function concentrated on Γ_0 [5,6,21,22,28], (4) is equal to I_0 analytically. Errors are therefore due only to the numerical scheme used to discretize (4) instead of both the numerical scheme and the anterior approximation.

For smooth curves or surfaces, the integral formulation (4) is very powerful: it provides a very elegant, simple and attractive computational method for computing surface integrals. In addition, the authors in [8] showed that the Jacobian can be expressed as the product of the nonzero singular values of the Jacobian matrix of the closest point mapping P_{Γ_0}. The benefit of such an expression is that for smooth integrands and smooth curves or surfaces, the accuracy of the discretizations of (4) will depend only on the order of the finite difference scheme used to approximate the Jacobian matrix of P_{Γ_0}.

Finally, we remark that if one has a level set function ϕ which is not the signed distance function to Γ_0, fast algorithms such as fast marching and fast sweeping [4,15,19,23,24] can be used to construct a signed distance function d to Γ_0.

2.2. **Computational difficulties near a corner.** Both Type I and Type II methods have difficulties resolving singularities from only the values of $\phi_{\mathbf{i}}$. In particular, Type II methods using the regularization parameter ϵ lead to $O(\epsilon)$ error for each corner. This error is partially due to the discretization of the Jacobian term. The new approach discussed in this paper does not use the Jacobian term and as such gives a viable approach to handling integrable singularities.

The particular approach described in [7,8] has specific difficulties in resolving the singularities. Indeed, in a neighborhood of a singular point, the change of variables (5) breaks down. This occurs whenever the signed distance function is not $C^{1,\alpha}, \alpha > 1$, and when the reach of the distance function is smaller than the tubular neighborhood $\{\mathbf{x} : -\epsilon \leq d(\mathbf{x}) \leq \epsilon\}$ (the reach refers to the region near Γ_0 where d is differentiable). In addition, since the expression for the Jacobian J involves curvatures of level sets, it will be necessary to use one-sided differencing to discretize J in order to avoid differentiating d across kinks. Finally, if we consider

a corner in two dimensions (see Figure 1) we see that in the convex region enclosed by Γ_0 near the corner point, points on an η-level set will not project onto the entire curve Γ_0, whereas points on the $(-\eta)$-level set will all project onto Γ_0, leading to a "deficiency" of points coming from one side.

A characterization of corners and edges via the closest point projection.
Let us now use the closest point mapping with distance η more explicitly as $P_\eta(\mathbf{x}) := \mathbf{x} - \eta\nabla d(\mathbf{x})$. One way to circumvent this "deficiency" issue is to identify the points on the $(-\eta)$-level set that project onto the part of Γ_0 that is missed by projecting the points from the η level set. Such points satisfy

$$(6) \qquad P_{-\eta}(P_{2\eta}(\mathbf{x})) \neq P_\eta(\mathbf{x}), \eta = d(\mathbf{x}),$$

which states that if we over project $\mathbf{x}$ by a distance 2η and then project the result back by a distance η (in the opposite direction), we are not back at the same point. Points away from the corner, on the other hand, i.e., in smooth regions, satisfy $P_{-\eta}(P_{2\eta}(\mathbf{x})) = P_\eta(\mathbf{x})$. (See Figure 1.)
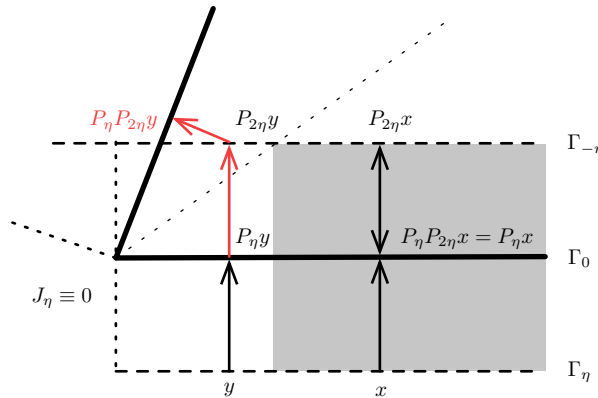

FIGURE 1. Projection near a corner.

Thus, once we have identified the points that satisfy (6), we count these points twice to compensate for the fact that these points have no corresponding ones on the η level set. This effectively translates into the following correction integral:

$$\int_{\mathbb{R}^2} f(P_\Gamma(\mathbf{x}))\omega(\mathbf{x})\delta_\epsilon(d(\mathbf{x}))d\mathbf{x},$$

with the weight ω defined as

$$\omega(\mathbf{x}) = \begin{cases} 0 & |d(\mathbf{x})\Delta d(\mathbf{x})| = 1, \\ 2 & P_{-\eta}(P_{2\eta}(\mathbf{x})) = P_\eta(\mathbf{x}), \eta = d(\mathbf{x}), \\ 1 & \text{otherwise.} \end{cases}$$

There are several issues with this approach: the first one is that the modification of the integrand with the weight ω leads to a discontinuous integrand. Thus the numerical approximation of the integral will not be able to reach a high order of accuracy. Second, there are numerical difficulties in the implementation of criteria (6): numerically, this requires the use of a threshold, which in turn raises the

question of how to choose such a threshold value. Thus, this approach is not suitable for high accuracy and does not provide a seamless implementation.

The purpose of the present work is to give an alternative but related integral formulation that allows the computations of surface integrals where the curve or surface has singular points, and which does not suffer from the issues discussed above. A large advantage of the new approach compared to (4) is that the new formulation does not involve the Jacobian J and is therefore more convenient to use. Additionally, it provides a mathematical understanding of the relationship between accuracy and how severe a singularity is.

3. The extrapolative approach

We now present the new approach which explores the smoothly varying relations among the different level sets of ϕ near Γ_0. In particular, for surfaces having corners, the integration of the nearby parallel surfaces varies smoothly as a function of the distance to the surface Γ_0, except at distance 0 (corresponding to the integral on Γ_0). Hence, it is possible to use kernels having suitable properties to approximate integration on Γ_0 by *extrapolating* integrations defined on other nearby surfaces.

3.1. **Smooth curves and surfaces.** Let $\phi : \mathbb{R}^n \mapsto \mathbb{R}$, $n \in \mathbb{N}$, be a Lipschitz function and let $\Gamma_\eta := \{\mathbf{x} : \phi(\mathbf{x}) = \eta\}$ be the η-level set of ϕ. We consider $\tilde{f} : \mathbb{R}^n \mapsto \mathbb{R}$ to be a Lipschitz function and define S as

$$(7) \qquad S := \int_{\mathbb{R}^n} \tilde{f}(\mathbf{x}) \delta_\epsilon(\phi(\mathbf{x})) |\nabla \phi(\mathbf{x})| d\mathbf{x}.$$

Integrals of the form (7) have been used to approximate I_0 but unlike (4), which coincides exactly with I_0, we have in general $S \approx I_0$. However, under specific conditions which we explain below, it is possible to have $S = I_0$ or to know precisely how the error between S and I_0 behaves in terms of ϵ (width of the tubular neighborhood around Γ_0) for example, and in terms of a corner or how sharp a cusp is.

We define the one-parameter family of functionals

$$(8) \qquad I[\tilde{f}, \phi](\eta) := \int_{\Gamma_\eta} \tilde{f}(\mathbf{x}) dS(\mathbf{x}),$$

which represents the integral of $\tilde{f}$ over the η-level set of ϕ. It is worth pointing out that in [7, 8], the authors considered a similar approach to construct (4), but their family of functionals was $F_\eta := \int_{\Gamma_\eta} \tilde{f}(\mathbf{x}) J_\eta(\mathbf{x}) dS(\mathbf{x})$, where the Jacobian J_η is the same as the Jacobian J in (4). The purpose of this Jacobian was to ensure the equality $F_\eta = I_0$ for all $-\epsilon \leq \eta \leq \epsilon$. In other words, I_0 was parameterized in terms of the nearby level sets within the tubular neighborhood. Unlike this original approach, (8) is not equal to I_0 for any η since there is no Jacobian term to compensate for the change in curvature. Now by the coarea formula, we can average over the parameterizations (8) using an averaging kernel δ_ϵ to obtain

$$(9) \qquad \int_{-\epsilon}^{\epsilon} \delta_\epsilon(\eta) I[\tilde{f}, \phi](\eta) d\eta = \int_{\mathbb{R}^n} \tilde{f}(\mathbf{x}) \delta_\epsilon(\phi(\mathbf{x})) |\nabla \phi(\mathbf{x})| d\mathbf{x} = S.$$

We then have the following result.

Theorem 1. *Suppose that:*
    (1) *d is the signed distance function to Γ_0, i.e., $|\nabla d| = 1$.*

(2) $\nabla \tilde{f} \cdot \nabla d = 0$ *in the viscosity solution sense, meaning that $\tilde{f}$ is constant along the normals of Γ_0 wherever normals are well defined (namely $\tilde{f}$ is the constant extension of $f : \Gamma_0 \mapsto \mathbb{R}$ along the normals of Γ_0).*

(3) Γ_η *are closed C^2 hypersurfaces for $-\epsilon \leq \eta \leq \epsilon$.*

Then for sufficiently small $\epsilon > 0$ such that $\Gamma_{\pm \epsilon} \neq \emptyset$, we have

$$I[\tilde{f}, d](\eta) = I_0 + \sum_{i=1}^{n-1} A_i \eta^i,$$

where A_i, $1 \leq i \leq n$ are constants that depend on $\tilde{f}$ and d.

Proof. Let us denote the closest point mapping to Γ_η (a.k.a the projection operator onto Γ_η) as $P_{\Gamma_\eta} : \mathbb{R}^n \mapsto \Gamma_\eta$. $\Gamma_\eta \in C^2$ for all $-\epsilon \leq \eta \leq \epsilon$, $\epsilon > 0$, then

$$I[\tilde{f}, d](\eta) = \int_{\Gamma_\eta} \tilde{f}(\mathbf{x}) dS(\mathbf{x})$$

$$= \int_{\Gamma_0} \tilde{f}(P_{\Gamma_\eta}(\mathbf{x})) \mathcal{J}_\eta(\mathbf{x}) dS(\mathbf{x}),$$

where $\mathcal{J}_\eta$ is the Jacobian that accounts for the change in curvature between Γ_η and Γ_0. Using the standard identity $\mathcal{J}_\eta = 1 + \sum_{i=1}^{n-1} \sigma_i(h) \eta^i$, where $\sigma_i(h)$ is the symmetric polynomial in the eigenvalues of the Weingarten map induced by the second fundamental form h associated to Γ_η; see [7] for a quick derivation. Thus we have

$$I[\tilde{f}, d](\eta) = \int_{\Gamma_0} \tilde{f}(P_{\Gamma_\eta}(\mathbf{x})) \left(1 + \sum_{i=1}^{n-1} \sigma_i(h) \eta^i \right) dS(\mathbf{x})$$

$$= \int_{\Gamma_0} \tilde{f}(P_{\Gamma_\eta}(\mathbf{x})) dS(\mathbf{x}) + \sum_{i=1}^{n-1} \eta^i \int_{\Gamma_0} \tilde{f}(P_{\Gamma_\eta}(\mathbf{x})) \sigma_i(h) dS(\mathbf{x})$$

$$= \int_{\Gamma_0} f(x) dS(\mathbf{x}) + \sum_{i=1}^{n-1} \left(\int_{\Gamma_0} \tilde{f}(P_{\Gamma_\eta}(\mathbf{x})) \sigma_i(h) dS(\mathbf{x}) \right) \eta^i$$

$$= I_0 + \sum_{i=1}^{n-1} A_i \eta^i,$$

where $A_i = \int_{\Gamma_0} \tilde{f}(P_{\Gamma_\eta}(\mathbf{x})) \sigma_i(h) dS(\mathbf{x})$, $1 \leq i \leq n$, and $I_0 = \int_{\Gamma_0} \tilde{f}(P_{\Gamma_\eta}(\mathbf{x})) dS(\mathbf{x})$ since $\tilde{f}$ is constant along the normals to Γ_0, and P_{Γ_η} is the orthogonal projection onto Γ_η, leading to $\tilde{f}(P_{\Gamma_\eta}(\mathbf{x})) = f(\mathbf{x})$ for all $\mathbf{x} \in \Gamma_0$. $\square$

This leads to the following generalization.

Corollary 2. *Assume now that the level set function ϕ is given by $\phi(\mathbf{x}) = \psi(d(\mathbf{x}))$, where d is the signed distance function to Γ_0 and $\psi : \mathbb{R} \to \mathbb{R}$ is a strictly monotonic function in $[-\epsilon, \epsilon]$, $\epsilon > 0$ satisfying $\psi(0) = 0$. Then*

$$I[\tilde{f}, \phi](\eta) = I_0 + \sum_{i=1}^{n-1} B_i \left(\psi^{-1}(\eta) \right)^i,$$

where $B_i, 1 \leq i \leq n$ are constants that depend on $\tilde{f}$ and ϕ.

Proof. Let $-\epsilon \leq \eta \leq \epsilon$ and let $\Gamma_\eta = \{\mathbf{x} : \phi(\mathbf{x}) = \eta\}$. Since ψ is strictly monotone in $[-\epsilon, \epsilon]$, ψ is invertible such that $\Gamma_\eta = \{\mathbf{x} : \psi(d(\mathbf{x})) = \eta\} = \{\mathbf{x} : d(\mathbf{x}) = \psi^{-1}(\eta)\} = \{\mathbf{x} : d(\mathbf{x}) = \xi\}$, where $\xi = \psi^{-1}(\eta)$ and d is the signed distance function to Γ_0. Thus

$$
\begin{aligned}
I[\tilde{f}, \phi](\eta) &= \int_{\Gamma_\eta} \tilde{f}(\mathbf{x}) dS(\mathbf{x}) \\
&= \int_{\Gamma_\xi} \tilde{f}(\mathbf{x}) dS(\mathbf{x}) \\
&= I[\tilde{f}, d](\xi) \\
&= I_0 + \sum_{i=1}^{n-1} B_i \xi^i,
\end{aligned}
$$

by using Theorem 1. Therefore,

$$
I[\tilde{f}, \phi](\eta) = I_0 + \sum_{i=1}^{n-1} B_i \left(\psi^{-1}(\eta) \right)^i,
$$

where $B_i = \int_{\Gamma_0} \tilde{f}(P_{\Gamma_\xi}) \sigma_i(h) dS(\mathbf{x})$, $1 \leq i \leq n$ with $\xi = \psi^{-1}(\eta)$. $\qquad\square$

An example of such a level set function is $\phi(\mathbf{x}) = d(\mathbf{x})^3$ or $\phi(\mathbf{x}) = \text{sgn}(d) d^2(\mathbf{x})$, where d is the signed distance function to Γ_0. We note that in these two examples, the expansion in η in $I[\tilde{f}, \phi](\eta)$ will include fractional powers of η; Indeed, if $\phi(\mathbf{x}) = d(\mathbf{x})^3$, then $\xi = \eta^{\frac{1}{3}}$ and thus

$$
I[\tilde{f}, \phi](\eta) = I_0 + \sum_{i=1}^{n-1} B_i \eta^{\frac{i}{3}}.
$$

In the dimensions of interest ($n = 2, 3$), Theorem 1 states that if Γ_0 is C^2, $\tilde{f}$ is constant along the normals of Γ_0 and d is the signed distance function to Γ_0, then $I[\tilde{f}, d]$ is linear in η for curves in two dimensions and quadratic in η for surfaces in three dimensions. Therefore, if we average the parameterizations $I[\tilde{f}, d]$ with a kernel δ_ϵ that has enough vanishing moments, the terms in η will vanish and we will be left with I_0, thus making $S = I_0$. The result is stated in the following theorem.

Theorem 3. *Assume that Theorem 1 holds and assume that the averaging kernel δ_ϵ is compactly supported in $[-\epsilon, \epsilon]$ with $n - 1$ vanishing moments (where n is the dimension), namely*

$$
\int_{-\infty}^{\infty} \delta_\epsilon(\eta) \eta^p d\eta = \begin{cases} 1 & p = 0, \\ 0 & 0 < p \leq n - 1, \end{cases}
$$

then

$$
I_0 = \int_{\Gamma_0} f(x) dS(x) = \int_{\mathbb{R}^n} \tilde{f}(\mathbf{x}) \delta_\epsilon(d(\mathbf{x})) d\mathbf{x} = S.
$$

Proof. Using (9), the result of Theorem (4) and the assumptions on δ_ϵ, we have

$$
\begin{aligned}
S &= \int_{-\epsilon}^{\epsilon} \delta_\epsilon(\eta) I[\tilde{f}, d](\eta) d\eta = \int_{-\epsilon}^{\epsilon} \delta_\epsilon(\eta) \left(I_0 + \sum_{i=1}^{n-1} A_i \eta^i \right) d\eta \\
&= I_0 \int_{-\infty}^{\infty} \delta_\epsilon(\eta) d\eta + \sum_{i=1}^{n-1} A_i \int_{-\infty}^{\infty} \delta_\epsilon(\eta) \eta^i d\eta = I_0. \qquad\square
\end{aligned}
$$

The main upshot of this result is that if the curve or surface is smooth (i.e., C^2), it is possible to construct S such that it coincides exactly with I_0. To be more specific, if the kernel δ_ϵ has enough vanishing moments, then $S = I_0$. For the dimensions of interest (2 and 3), it is easy to construct kernels with 1 or 2 vanishing moments. For large dimensions, we point out that it might not be easy to construct a kernel with enough vanishing moments to obtain the equality between S and I_0, but in that case, the error between S and I_0 will be related to the number of vanishing moments of δ_ϵ. Thus, the higher the number of vanishing moments, the more accurate the approximation S will be to I_0.

Note that in general, $I[\tilde{f}, d]$ may not be a polynomial in η, but as long as $I[\tilde{f}, d]$ has a Taylor expansion about $\eta = 0$, the accuracy of using S to approximate I_0 will be determined by the number of vanishing moments of the kernel δ_ϵ. Also in the case of a general level set function ϕ, $I[\tilde{f}, \phi]$ will have an expansion with fractional powers of η, thus requiring a special class of kernels with "fractional" vanishing moments in order to expect S to coincide exactly with I_0. This, highlights that for smooth interfaces, it is advantageous to use a signed distance function.

Theorem 3 has several implications. First, it is very convenient to use because unlike (4), this formulation does not need the Jacobian term. It is therefore simpler to implement and it performs the same as (4) *as long as the kernel is chosen appropriately.* In a way, this can be understood as a trade-off between number of vanishing moments and the Jacobian. The Jacobian allows (4) to be exact, but S can be made exact by using a kernel with enough vanishing moments. Second, this simpler formulation gives a viable approach for approximating integrals over curves and surfaces with singularities.

3.2. Curves with corners.
In this section, we assume that Γ_0 is a piecewise C^2 closed curve in $\mathbb{R}^2$ with a corner at (x_0, y_0). This includes a smooth closed parameterized curve that intersects itself at (x_0, y_0). The purpose of this section is to study the behavior of $I[\tilde{f}, \phi](\eta)$ as a function of η around $\eta = 0$ in order to deduce how the error incurred between S and I_0 depends on the type of singularity (corner or cusp). We describe the corner/cusp as follows:

- Corner. We consider a function $g : [0, \infty) \mapsto [0, \infty)$ such that $g(0) = 0$ and for $x > 0$, g is C^2 with $g'(0) > 0$.
- Cusp. We consider a function $g : [0, \infty) \mapsto [0, \infty)$ such that $g^{(\nu)}(0) = 0$ for $0 \leq \nu < p$ ($p \in \mathbb{N}, p \geq 2$) and $g^{(p)}(0) > 0$.

We consider the part of Γ_0 around the corner to be defined by the union of the graphs of g and $-g$. In this case, both sides of the x-axis contribute the same amount of "singularity". In the general case, where the corner is likely not symmetric about the x-axis, the error will be dominated by the most "singular side".

In this new coordinate system, the corner is at $(0,0)$. We then parameterize the part of Γ_0 that lies above the x-axis by

$$\gamma(x) := \begin{pmatrix} x \\ g(x) \end{pmatrix},$$

as shown in Figure 2. In this setup, the distance function to Γ_0 is differentiable away from the positive x-axis.

Define the normal to γ by

$$\vec{n}(x) = \frac{1}{\sqrt{1 + g'(x)^2}} \begin{pmatrix} g'(x) \\ -1 \end{pmatrix}$$

and consider the lines

$$L(\eta; x) := \gamma(x) + \eta \vec{n}(x),$$

which correspond to the characteristics of the Eikonal equation that emanates from γ before they intersect the x-axis. We first find η such that $L(\eta, x)$ intersects the x-axis, i.e.,

$$\begin{pmatrix} x \\ g(x) \end{pmatrix} + \frac{\eta}{\sqrt{1 + g'(x)^2}} \begin{pmatrix} g'(x) \\ -1 \end{pmatrix} = \begin{pmatrix} X_\eta \\ 0 \end{pmatrix},$$

where X_η is the x-coordinate of the intersection point between the η-level set and the x-axis. (See Figure 2.)
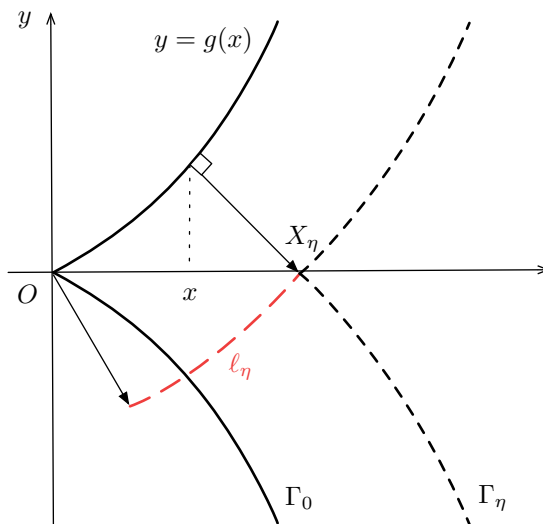

FIGURE 2. An illustration of a curve with a corner/cusp and a curve which is η distance away from it.

Using the information from the y-coordinates in the above vector equation we obtain

$$(10) \qquad \eta = g(x)\sqrt{1 + g'(x)^2} := F(x).$$

Thus, the $\eta(x)$-level set of the signed distance function to Γ_0 has a corner or cusp at $(X_\eta, 0)$. Now we estimate the length of the portion of Γ_0, the projection of which to the $\eta(x)$-level set is missing, denoted by $l(x)$ and given by

$$(11) \qquad l(x) = \int_0^x \sqrt{1 + g'(s)} \, ds.$$

If we now look at the integration of $\tilde{f}$ over a portion of the η-level set of d above the x-axis, we are missing the corresponding integral

$$l_{\eta(x)}^+[\tilde{f}, d] = \int_0^{x(\eta)} \tilde{f}(s, g(s))\sqrt{1 + g'(s)^2} J_s \, ds,$$

where $J_s = (1 + \eta \kappa(s))$ is the Jacobian that accounts for the change in curvature between Γ_0 and Γ_η (see [7]). In this integral, we are integrating over the portion of Γ_η that would be there if there was no corner (represented by the long dashed curve in Figure 2). The term $\sqrt{1 + g'(s)^2}ds$ is the arclength along Γ_0, and the term $\sqrt{1 + g'(s)^2}J_s ds$ is the arclength along Γ_η. It follows that we have

$$
\begin{aligned}
l^+_{\eta(x)}[\tilde{f}, d] &= \int_0^{x(\eta)} \tilde{f}(s, g(s))(1 + \eta \kappa(s))\sqrt{1 + g'(s)^2}ds \\
&= \int_0^{x(\eta)} \tilde{f}(s, g(s))\sqrt{1 + g'(s)^2}ds + \eta \int_0^{x(\eta)} \tilde{f}(s, g(s))\kappa(s)\sqrt{1 + g'(s)^2}ds \\
&= A^+(x(\eta)) + \eta B^+(x(\eta)),
\end{aligned}
$$

where $\kappa(s)$ is the curvature of Γ_0 at the point $(s, g(s))$, and $x(\eta) = F^{-1}(\eta)$, where F is given in (10) and F is invertible around $x = 0$. The invertibility of F is proven in Lemma 6. Away from the corner, the curve is smooth and therefore the error between S and I_0 is dominated by the effect of the corner. We choose to focus on the corner for $x \in [0, b]$, $b > 0$. (See Figure 3.)
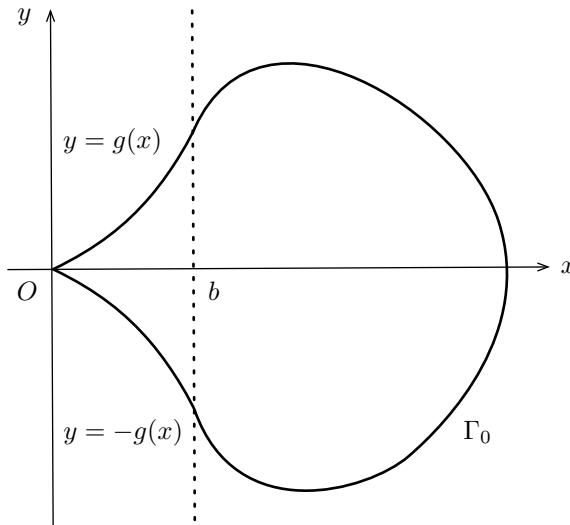

FIGURE 3. The closed curve Γ_0 with a corner at $(0, 0)$.

Thus the integral over one side of the corner (above the x-axis) is

$$
\begin{aligned}
G^+_\eta &= \int_0^b \tilde{f}(s, g(s))(1 + \eta \kappa(s))\sqrt{1 + g'(s)^2}ds \\
&= \int_0^{x(\eta)} \tilde{f}(s, g(s))(1 + \eta \kappa(s))\sqrt{1 + g'(s)^2}ds \\
&\quad + \int_{x(\eta)}^b \tilde{f}(s, g(s))(1 + \eta \kappa(s))\sqrt{1 + g'(s)^2}ds \\
&= l^+_\eta + I^+_\eta,
\end{aligned}
$$

where I_η^+ is the integration of $\tilde{f}$ along the portion of Γ_η above the x-axis. Thus

$$I_\eta^+ = G_\eta^+ - l_\eta^+ = G_\eta^+ - A^+(x(\eta)) - \eta B^+(x(\eta)).$$

The result for the integral along the portion of Γ_η below the x-axis is obtained similarly and thus

$$I_\eta^- = G_\eta^- - l_\eta^- = G_\eta^- - A^-(x(\eta)) - \eta B^-(x(\eta)),$$

with

$$A^-(x(\eta)) = \int_0^{x(\eta)} \tilde{f}(s, -g(s))\sqrt{1 + g'(s)^2}ds,$$

$$B^-(x(\eta)) = \int_0^{x(\eta)} \tilde{f}(s, -g(s))\kappa(s)\sqrt{1 + g'(s)^2}ds.$$

We point out that l_η^+ and l_η^- are no longer polynomials in η. WLOG, we assume that Γ_0 has only one corner and we denote by $\mathcal{P}_\eta^+$ and $\mathcal{P}_\eta^-$ the portion of Γ_η above the x-axis and below the x-axis, respectively. By construction, the term $G_\eta^+ + G_\eta^- + \int_{\Gamma_0 \setminus (\mathcal{P}_\eta^+ \cup \mathcal{P}_\eta^-)} \tilde{f}(\mathbf{x})dS(\mathbf{x})$ no longer has a corner. Thus we can apply Theorem 1 and obtain

$$(12) \qquad G_\eta^+ + G_\eta^- + \int_{\Gamma_0 \setminus (\mathcal{P}_\eta^+ \cup \mathcal{P}_\eta^-)} \tilde{f}(\mathbf{x})dS(\mathbf{x}) = I_0 + A\eta, \ A \in \mathbb{R},$$

which is equivalent to

$$(13) \qquad I[\tilde{f}, d](\eta) := I_\eta^+ + I_\eta^- + \int_{\Gamma_0 \setminus (\mathcal{P}_\eta^+ \cup \mathcal{P}_\eta^-)} \tilde{f}(\mathbf{x})dS(\mathbf{x}) = I_0 + A\eta - l_\eta^+ - l_\eta^-.$$

Note that the expression for the constant A in (12) can be obtained by using the expressions for the constants A_i given in the proof of Theorem 1.

Not surprisingly, it turns out that there is a fundamental difference in integration of parallel surfaces near a corner and near a cusp on Γ_0.

Theorem 4. *Consider a curve Γ_0 in $\mathbb{R}^2$ such that Γ_0 has a corner at (x_0, y_0). Let d be the signed distance function to Γ_0 used to compute S. Assume $f \in C^0(\Gamma_0)$ and that the curvature κ is continuous everywhere except at the corner point. Assume that $g \in C^2([0, \infty), [0, \infty))$ with $g(0) = 0$ and for $p \in \mathbb{N}$, $g^{(\nu)}(0) = 0$ for $0 \leq \nu < p$ and $g^{(p)}(0) > 0$, such that the corner/cusp is modeled by the graphs of g and $-g$. In this new coordinate system, the corner/cusp is at $(0, 0)$. Suppose also that the averaging kernel δ_ϵ is compactly supported in $[-\epsilon, \epsilon]$ with m vanishing moments such that*

$$\delta_\epsilon(\eta) = O(\epsilon^{-k})$$

as $\eta \to 0$, $(k \in \mathbb{N})$. Then

$$|S - I_0| = \begin{cases} O\left(\epsilon^{2+m-k}\right) & p = 1 \ (corner), \\ O\left(\epsilon^{1+\frac{1}{p}-k}\right) & p \geq 2 \ (cusp) \end{cases}$$

for small $\epsilon > 0$.

Note that the number of vanishing moments of the kernel δ_ϵ only plays a role in the case of a corner. For cusps, it is necessary to construct a different class of kernels that integrate to zero when multiplied by fractional powers of η.

4. Proof of Theorem 4

We start with two technical lemmas that are needed to complete the proof of Theorem 4 and then give the proof of Theorem 4.

Lemma 5. *Suppose $p \in \mathbb{N}$, and assume that $k : [0, \infty) \mapsto \mathbb{R}$ can be expressed as $k(x) = cx^{\gamma} + \iota(x)$ with $\gamma > p$, $c \in \mathbb{R}$ and $\lim_{x \to 0} \frac{\iota(x)}{x^{\gamma}} = 0$.*
Then if $\alpha_p > 0$, the series

$$\sum_{n=0}^{\infty} \binom{\frac{1}{p}}{n} \left(\frac{k(x)}{\alpha_p x^p} \right)^n$$

is uniformly convergent for $x \in [0, r)$ for some $r > 0$.

Proof. The assumptions on k imply that $\lim_{x \to 0} \frac{k(x)}{x^p} = 0$. Thus, there exists $r_0 > 0$ such that

$$(14) \qquad \left| \frac{k(x)}{\alpha_p x^p} \right| = \frac{k(x)}{\alpha_p x^p} < 1 \text{ on } x \in [0, r_0).$$

In addition, since $x \mapsto \frac{k(x)}{x^p}$ is dominated by cx^{γ} in a neighborhood of 0, it follows that in a neighborhood of 0, the function $x \mapsto \frac{k(x)}{x^p}$ behaves the same as cx^{γ} and thus is increasing around 0. It follows that there exists $r_1 > 0$ such that for all $0 < x < y < r_1$,

$$(15) \qquad 0 < \frac{k(x)}{x^p} < \frac{k(y)}{y^p}.$$

We define $r = \min(r_0, r_1)$.
Since

$$\left| \binom{\frac{1}{p}}{n} \right| \left| \frac{k(x)}{\alpha_p x^p} \right|^n \leq \left| \frac{k(x)}{\alpha_p x^p} \right|^n$$

the series is convergent for $x \in [0, r)$. This inequality comes from the fact that the sequence $\left| \binom{\frac{1}{p}}{n} \right|$ is decreasing in n, which we prove at the end.

We now show that the series is uniformly convergent in that interval. Pick $0 < \rho < r$. Then for $0 < x < \rho < r$, we have by (15) and (14)

$$0 < \frac{k(x)}{x^p} < \frac{k(\rho)}{\rho^p} < \alpha_p.$$

Thus we have

$$\left| \binom{\frac{1}{p}}{n} \left(\frac{k(x)}{\alpha_p x^p} \right)^n \right| < \left| \binom{\frac{1}{p}}{n} \frac{k(\rho)}{\alpha_p \rho^p}^n \right| := \left| \binom{\frac{1}{p}}{n} \right| \zeta^n \leq \zeta^n,$$

with $0 < \zeta < 1$. Consequently, the series $\sum_{n=0}^{\infty} |\binom{\frac{1}{p}}{n}| \zeta^n$ converges. Thus by the Weierstrass M-test, it follows that the series converges uniformly for $0 \leq x < \rho$. Since ρ is arbitrary in $[0, r)$, the series converges uniformly on $[0, r)$.

We now show that the sequence $\left| \binom{\frac{1}{p}}{n} \right|$ is decreasing in n. Let $u_n^p := \left| \binom{\frac{1}{p}}{n} \right|$. For $p = 1$, we have $u_0^1 = u_1^1 = 1$ and $u_n^1 = 0$ for $n \geq 2$. Thus, for all $n \geq 0, u_n^1 \leq 1$. Now, consider $p \geq 2$. By definition of the sequence, we have

$$\forall k \in \mathbb{N}, \binom{\frac{1}{p}}{2k} = -u_{2k}^p \leq 0, u_{2k-1}^p \geq 0.$$

For $k \geq 1$, we have

$$u^p_{2k+1} - u^p_{2k} = \frac{\frac{1}{p}(\frac{1}{p} - 1)(\frac{1}{p} - 2) \cdots (\frac{1}{p} - 2k)}{(2k+1)!} - \frac{-\frac{1}{p}(\frac{1}{p} - 1)(\frac{1}{p} - 2) \cdots (\frac{1}{p} - 2k + 1)}{(2k)!}$$

$$= \frac{\frac{1}{p}(\frac{1}{p} - 1)(\frac{1}{p} - 2) \cdots (\frac{1}{p} - 2k + 1)}{(2k)!} \left(1 + \frac{\frac{1}{p} - 2k}{2k+1}\right)$$

$$= \frac{\frac{1}{p}(\frac{1}{p} - 1)(\frac{1}{p} - 2) \cdots (\frac{1}{p} - 2k + 1)}{(2k)!} \left(\frac{1 + \frac{1}{p}}{2k+1}\right) < 0,$$

since the numerator of the first fraction is the product of an even number of terms, and thus is negative.

Similarly, for $k \geq 1$, we have

$$u^p_{2k} - u^p_{2k-1} = \frac{\frac{1}{p}(\frac{1}{p} - 1)(\frac{1}{p} - 2) \cdots (\frac{1}{p} - 2k + 2)}{(2k-1)!} \left(-\frac{\frac{1}{p} + 1}{2k}\right) < 0,$$

since the numerator in the first fraction is the product of an odd number of terms, which is positive. Thus

$$\forall n \geq 1, p \geq 1, u^p_{n+1} - u^p_n \leq 0.$$

Since $u^p_0 = 1, \forall p \geq 1$ and $u^p_1 = \frac{1}{p}, \forall p \geq 1$, it follows that

$$\forall n \geq 0, p \geq 1, u^p_{n+1} - u^p_n \leq 0.$$

Thus the sequence is decreasing and bounded above by its first term, which is 1. $\quad\square$

Lemma 6. *Assume that $g \in C^2([0, \infty), [0, \infty))$ with $g(0) = 0$, and for $p \in \mathbb{N}$, $g^{(\nu)}(0) = 0$ for $0 \leq \nu < p$ and $g^{(p)}(0) > 0$. Let $F : [0, \infty) \mapsto [0, \infty)$ be defined as $F(x) = g(x)\sqrt{1 + g'(x)^2}$. Then locally around $x = 0$, F is invertible and $F(x) = ax^p + o(x^p)$ as $x \to 0$ $(a \in \mathbb{R} \setminus \{0\})$ with $p \in \mathbb{N}$, and*

$$x(\eta) = F^{-1}(\eta) = \left(\frac{\eta}{a}\right)^{\frac{1}{p}} + o(\eta^{\frac{1}{p}})$$

as $\eta \to 0$.

Proof. Since $g \in C^2([0, \infty))$, then $F(x) = g(x)\sqrt{1 + g'(x)^2}$ is in $C^1([0, \infty))$, with

$$F'(x) = \frac{g'(x)(1 + g'(x)^2) + g(x)g'(x)g''(x)}{\sqrt{1 + g'(x)^2}} = \frac{g'(x)}{\sqrt{1 + g'(x)^2}}(1 + g'(x)^2 + g(x)g''(x)).$$

- Case 1. Corner case: suppose $g'(0) > 0$. Then $F'(0) = \frac{g'(0)(1+g'(0)^2)}{\sqrt{1+g'(0)^2}} > 0$.
  Since F' is continuous on $[0, \infty)$, one can find a neighborhood of $x = 0$, $[0, \nu)$ (for some $\nu > 0$), such that for all $x \in [0, \nu)$, we have $F'(x) > 0$. Thus, F is strictly increasing on $[0, \nu)$ and therefore invertible on $[0, \nu)$, i.e.,

$$\forall x \in [0, \nu), x = F^{-1}(\eta)$$

  with $F^{-1}(0) = 0$ (since $g(0) = 0 \Rightarrow F(0) = 0$). Since $F \in C^1([0, \infty))$ with $F'(0) > 0$, it follows that F can be written as

$$F(x) = a_1 x + q(x),$$

where $a_1 = F'(0) > 0$, and $\lim_{x \to 0} \frac{q(x)}{x} = 0$. Thus $F(x) = a_1 x + o(x)$ as $x \to 0$ with $a_1 \neq 0$. Let us look for its local inverse around $x = 0$, F^{-1}, as

(16)
$$F^{-1}(\eta) = b_1 \eta + h(\eta),$$

such that $\lim_{\eta \to 0} \frac{h(\eta)}{\eta} = 0$. Then using $F^{-1}(F(x)) = x$ for $x \in [0, \nu)$, we obtain

$$\begin{aligned}
F^{-1}(F(x)) &= F^{-1}(a_1 x + q(x)) \\
&= b_1(a_1 x + q(x)) + h(a_1 x + q(x)) \\
&= a_1 b_1 x + b_1 q(x) + h(a_1 x + q(x)) \\
&= a_1 b_1 x + R(x),
\end{aligned}$$

where $R(x) = b_1 q(x) + h(a_1 x + q(x))$. If we choose $b_1 = \frac{1}{a_1}$, then for $x \in [0, \nu)$ we have

$$F^{-1}(F(x)) = x + R(x).$$

Now F^{-1} is the correct inverse if $R(x) = 0$, but we cannot know what R is since we do not have an expression for q and h. Nevertheless, asymptotically around $x = 0$, R needs to satisfy $\lim_{x \to 0} \frac{R(x)}{x} = 0$. Let us then calculate this limit:

$$\begin{aligned}
\lim_{x \to 0} \frac{R(x)}{x} &= \lim_{x \to 0} \frac{b_1 q(x) + h(a_1 x + q(x))}{x} \\
&= b_1 \lim_{x \to 0} \frac{q(x)}{x} + \lim_{x \to 0} \frac{h(a_1 x + q(x))}{x} \\
&= 0,
\end{aligned}$$

since $\lim_{x \to 0} \frac{q(x)}{x} = 0$ and $\lim_{x \to 0} \frac{h(a_1 x + q(x))}{x} = \lim_{y \to 0} \frac{h(y)}{y} = 0$ with $y = a_1 x + q(x) = a_1 x + o(x) \to \lim_{x \to 0} = 0$. Thus if the inverse F^{-1} is of the form (16), we have the correct asymptotic behavior for $F^{-1} \circ F$. By the unicity of the inverse, it follows that necessarily around $\eta = 0$ we have

$$F^{-1}(\eta) = \frac{\eta}{a_1} + h(\eta),$$

with $\lim_{\eta \to 0} \frac{h(\eta)}{\eta} = 0$.

- Case 2. Cusp case: Suppose $g^{(\nu)}(0) = 0$ for $0 \leq \nu < p$ ($p \in \mathbb{N}, p \geq 2$) and $g^{(p)}(0) > 0$. Then $F'(0) = 0$. First, we show that F is invertible, and to do so, we will show that $F'(x) > 0$ on an interval $(0, \mu)$ for some $\mu > 0$. Since $g \in C^2([0, \infty), [0, \infty))$ and satisfies $g(0) = g'(0) = 0$, it follows that in a neighborhood of 0, say $(0, \mu)$ for some $\mu > 0$, g is strictly increasing and concave up. Thus $F'(x) > 0$ on $(0, \mu)$ for some $\mu > 0$. We therefore conclude that F is invertible in a neighborhood of 0.

  Now since $g \in C^2([0, \infty), [0, \infty))$ with $g(0) = g'(0) = 0$, it follows that $F \in C^1([0, \infty), [0, \infty))$ with $F(0) = F'(0) = 0$. Let us assume that we can write F as

$$F(x) = \alpha_p x^p + k(x),$$

with $\alpha_p > 0$, and $k(x) = c x^\gamma + \iota(x)$ with $\gamma > p$, $c \in \mathbb{R}$ and $\lim_{x \to 0} \frac{\iota(x)}{x^\gamma} = 0$. Note that these assumptions imply that $\lim_{x \to 0} \frac{k(x)}{x^p} = 0$.

We then look for its local inverse F^{-1} as

$$F^{-1}(\eta) = \beta_1 \eta^{\frac{1}{p}} + w(\eta),$$

such that $\lim_{\eta \to 0} \frac{w(\eta)}{\eta^{\frac{1}{p}}} = 0$. Using $F^{-1}(F(x)) = x$ on $(0, \mu)$, we obtain

$$
\begin{aligned}
F^{-1}(F(x)) &= \beta_1 F(x)^{\frac{1}{p}} + w(F(x)) \\
&= \beta_1 (\alpha_p x^p + k(x))^{\frac{1}{p}} + w(\alpha_p x^p + k(x)) \\
&= \beta_1 \alpha_p^{\frac{1}{p}} x \sum_{n=0}^{\infty} \binom{\frac{1}{p}}{n} \left(\frac{k(x)}{\alpha_p x^p} \right)^n + w(\alpha_p x^p + k(x)) \\
&= \beta_1 \alpha_p^{\frac{1}{p}} x + T(x),
\end{aligned}
$$

where $T(x) = \beta_1 \alpha_p^{\frac{1}{p}} x \sum_{n=1}^{\infty} \binom{\frac{1}{p}}{n} \left(\frac{k(x)}{\alpha_p x^p} \right)^n + w(\alpha_p x^p + k(x))$. If we choose $\beta_1 = \alpha_p^{\frac{-1}{p}}$, then we have $F^{-1}(F(x)) = x + T(x)$. It remains to show that this gives the correct asymptotic behavior at $x = 0$, namely that $\lim_{x \to 0} \frac{T(x)}{x} = 0$.

$$
\begin{aligned}
\lim_{x \to 0} \frac{T(x)}{x} &= \lim_{x \to 0} \frac{\beta_1 \alpha_p^{\frac{1}{p}} x \sum_{n=1}^{\infty} \binom{\frac{1}{p}}{n} \left(\frac{k(x)}{\alpha_p x^p} \right)^n + w(\alpha_p x^p + k(x))}{x} \\
&= \beta_1 \alpha_p^{\frac{1}{p}} \lim_{x \to 0} \sum_{n=1}^{\infty} \binom{\frac{1}{p}}{n} \left(\frac{k(x)}{\alpha_p x^p} \right)^n + \lim_{x \to 0} \frac{w(\alpha_p x^p + k(x))}{x} \\
&= \beta_1 \alpha_p^{\frac{1}{p}} \sum_{n=1}^{\infty} \binom{\frac{1}{p}}{n} \frac{1}{\alpha_p^n} \lim_{x \to 0} \left(\frac{k(x)}{x^p} \right)^n + \lim_{x \to 0} \frac{w(\alpha_p x^p + k(x))}{x},
\end{aligned}
$$

where we have used the uniform convergence of the series $\sum_{n=1}^{\infty} \binom{\frac{1}{p}}{n} \left(\frac{k(x)}{\alpha_p x^p} \right)^n$ to interchange the sum and the limit by Lemma 5. Since $\lim_{x \to 0} \frac{k(x)}{x^p} = 0$ it follows that for all $n \geq 1$, we have $\lim_{x \to 0} \left(\frac{k(x)}{x^p} \right)^n = 0$. Additionally, $\lim_{x \to 0} \frac{w(\alpha_p x^p + k(x))}{x} = \lim_{y \to 0} \frac{w(y)}{y^{\frac{1}{p}}} = 0$ with $y = \alpha_p x^p + k(x) = O(x^p) \Rightarrow x = O(y^{\frac{1}{p}})$. Therefore $\lim_{x \to 0} \frac{T(x)}{x} = 0$, hence leading to the desired asymptotic behavior. Since the inverse is unique, it follows that asymptotically around $\eta = 0$ we have

$$F^{-1}(\eta) = \left(\frac{\eta}{\alpha_p} \right)^{\frac{1}{p}} + w(\eta),$$

where $\lim_{\eta \to 0} \frac{w(\eta)}{\eta^{\frac{1}{p}}} = 0$. $\qquad \square$

Proof of Theorem 4. As shown earlier we have for $\eta > 0$,

$$l_\eta^{\pm} = A^{\pm}(x(\eta)) + \eta B^{\pm}(x(\eta)).$$

Since f is continuous and κ is continuous everywhere except at the corner point, we have $f(s, \pm g(s))\sqrt{1 + g'(s)^2} = O(1)$ and $f(s, \pm g(s))\kappa(s)\sqrt{1 + g'(s)^2} = O(1)$ as $x \to 0$. Thus

$$A^{\pm}(x(\eta)) = \int_0^{x(\eta)} f(s, \pm g(s))\sqrt{1 + g'(s)^2}\,ds$$
$$= O(\eta^{\frac{1}{p}}) \text{ as } \eta \to 0^+$$

and

$$B^{\pm}(x(\eta)) = \int_0^{x(\eta)} f(s, \pm g(s))\kappa(s)\sqrt{1 + g'(s)^2}\,ds$$
$$= O(\eta^{\frac{1}{p}}) \text{ as } \eta \to 0^+$$

by using Lemma 6. Thus

$$l_\eta^{\pm} = O(\eta^{\frac{1}{p}}) \text{ as } \eta \to 0^+.$$

Therefore, using (13) , we have

$$I[\tilde{f}, d](\eta) = I_0 + O(\eta^{\frac{1}{p}}) \text{ as } \eta \to 0^+.$$

For $\eta < 0$, since everything is smooth on that side, we can apply Theorem 1 to obtain

$$I[\tilde{f}, d](\eta) = I_0 + O(\eta) \text{ as } \eta \to 0^-.$$

For $p = 1$, we have

$$S = \int_\epsilon^\epsilon I[\tilde{f}, d](\eta)\delta_\epsilon(\eta)d\eta$$
$$= \int_{-\epsilon}^\epsilon I_0 \delta_\epsilon(\eta)d\eta + O\left(\int_{-\epsilon}^\epsilon \eta\delta_\epsilon(\eta)d\eta\right)$$
$$= I_0 + O\left(\int_{-\epsilon}^\epsilon \eta\delta_\epsilon(\eta)d\eta\right).$$

In this case, $I[\tilde{f}, d](\eta)$ only contains integer powers of η (Taylor series). It follows that since δ_ϵ has m vanishing moments,

$$S = I_0 + O\left(\int_\epsilon^\epsilon \eta^{m+1}\delta_\epsilon(\eta)d\eta\right)$$
$$= I_0 + O\left(\epsilon^{-k}\int_{-\epsilon}^\epsilon \eta^{m+1}d\eta\right)$$
$$= I_0 + O(\epsilon^{m+2-k}).$$

For $p \geq 2$, we have

$$
\begin{aligned}
S &= \int_{-\epsilon}^{\epsilon} I[\tilde{f}, d](\eta)\delta_\epsilon(\eta)d\eta \\
&= \int_{-\epsilon}^{0} I[\tilde{f}, d](\eta)\delta_\epsilon(\eta)d\eta + \int_{0}^{\epsilon} I[\tilde{f}, d](\eta)\delta_\epsilon(\eta)d\eta \\
&= \int_{-\epsilon}^{\epsilon} I_0 \delta_\epsilon(\eta)d\eta + O\left(\int_{-\epsilon}^{0} \eta\delta_\epsilon(\eta)d\eta\right) + O\left(\int_{0}^{\epsilon} \eta^{\frac{1}{p}}\delta_\epsilon(\eta)d\eta\right) \\
&= I_0 + O\left(\epsilon^{-k}\int_{-\epsilon}^{0} \eta d\eta\right) + O\left(\epsilon^{-k}\int_{0}^{\epsilon} \eta^{\frac{1}{p}}d\eta\right) \\
&= I_0 + O(\epsilon^{-k+2}) + O(\epsilon^{-k+\frac{1}{p}+1}) \\
&= I_0 + O(\epsilon^{1+\frac{1}{p}-k}). \qquad\qquad\qquad\qquad\qquad\qquad\qquad \square
\end{aligned}
$$

5. Numerical simulations

In this section, we present a few numerical computations aiming at demonstrating the unique properties of the proposed approach to surface integrals using implicit representations. These properties include:

(1) High order approximations of smooth or piecewise smooth interfaces with the use of sufficiently regular level set functions.

(2) Analytically exact integrals and highly accurate numerical approximations with the help of a sufficiently regular level set function and constant-in-normal extensions of the integrands.

(3) The potential in computing singular integrals using uniform Cartesian grids.

These properties are the consequences of the use of special averaging kernels. The numerical computations presented in this section will involve the following kernels, constructed in [3]:

- A C^∞ kernel with one vanishing moment:

$$
\delta_{\infty,1}(r) := \exp\left(\frac{2}{(2r-1)^2 - 1}\right)(ar + b)\chi_{[0,1]}(r),
$$

$$
a = -261.5195892865372, \quad b = 145.7876577089403.
$$

- A C^∞ kernel with one vanishing moment:

$$
\delta_{\rho,\infty,1}(r) := \exp\left(\frac{1}{2(r^2 - 1)}\right)(a_\rho r + b_\rho)\chi_{[\rho,1]}(r).
$$

This kernel is designed specifically for integrands with an integrable singularity. The support of the kernel, which is ρ away from the singularity, is constructed to mitigate the effect of the singularity. In the following computations, ρ is taken to be 0.1, and

$$
a_{0.1} = -759.2781934172483, \quad b_{0.1} = 446.2604260472818.
$$

- A C^∞ kernel with two vanishing moments:

$$
\delta_{\infty,2}(r) := \exp\left(\frac{2}{(2r-1)^2 - 1}\right)(ar^2 + br + c)\chi_{[0,1]}(r),
$$

$$a = 3196.1015220946833, \quad b = -3457.6211113812255,$$
$$c = 852.9832518883903.$$

In the examples below, $\delta_\epsilon(\cdot)$ will be taken to be $\epsilon^{-1}\tilde{\delta}\left(\frac{\cdot}{\epsilon}\right)$, where $\tilde{\delta}$ is one of the kernels defined above. We use the Cartesian grids $h\mathbb{Z}^n \cap [-1, 1]^n$, $n = 2, 3$. The notation $\phi_{i,j}$ is used to denote the value of ϕ at the grid node (ih, jh). Similar notations are used for other functions. If ϕ is a distance function, we define $\nabla\phi(x, y) \equiv 1$. This is in fact an advantage of using distance functions to embed closed hypersurfaces. We will study the effect of the kernels with more general Lipschitz continuous level set functions. Since our focus is on the kernels, we will use analytically defined formulas for $\nabla\phi$ in the respective examples.

Let us briefly summarize what to observe in the following examples. The error computed by the proposed summation consists of two parts: one part is of analytical nature and depends on the number of vanishing moments of the kernel, as well as how

$$I[f, \phi](\eta) = \int_{\Gamma_\eta} f\, dS,$$

the one-parameter family of integrals, changes as a function of η. Here Γ_η is the η-level set of ϕ. If $I[f, \phi](\eta)$ is a quadratic polynomial in η for instance, then there is no error in the analytical approximation for a kernel with at least two vanishing moments. Otherwise, the analytical error will be proportional to ϵ^{m+1}, where m is the number of vanishing moments of the kernel.

The second part of the computed error is the accuracy of the discretization of the level set surface integral S, defined in (7). In the following examples, we propose the use of simple Riemann sums to discretize the integrand over the grid. Due to the compactness of the kernel, the integrand in (7) can be regarded as a periodic function defined on $[-1, 1]^n$, and thus the simple Riemann sum is equivalent to the Trapezoidal rule. Therefore, the discretization error inherits the convergence property of the Trapezoidal rule for periodic functions on uniform grids. Note that the regularity of the kernel greatly influences the discretization or quadrature error.

Finally, we pointed out that in practice, if ϕ is not a distance function, $\nabla\phi$ will need to be approximated on the grid. Typically, $\nabla\phi$ is approximated by simple central differencing yielding second order in h approximations or fifth order WENO approximations. Naturally the accuracy of the overall approximation of the surface integral will be affected. *In other words, we show that by a smart choice of kernel, we can eliminate many components of the errors associated to a typical approximation of (1) by discretization of (7) on uniform grids.*

Also in the examples below, we study the relative errors as functions of h, and present the observed rate at which the computed errors tend to 0 as h decreases. We shall scale ϵ according to different powers of h and observe that the computed error does decrease at the rate as predicted by the theory, when discretization errors are negligible (due to C_c^∞ kernels). Given the level set function on a uniform Cartesian grid with spacing h, the computational complexity of the proposed method is formally $O(N^{n-1}\frac{\epsilon}{h})$, where $\epsilon = O(h^r)$ for $0 < r \leq 1$, $h = O(\frac{1}{N})$ where N is the number of grid points in each coordinate direction, and n is the dimension of the embedding Euclidean space. Here the term N^{n-1} is the standard estimate of the number of points on the interface, and the additional factor ϵ/h gives the number of grid points used to resolve the kernel. In terms of N only, the computational

complexity becomes $O(N^{n-r})$. In the following examples, the global error is dominated by the analytical error due to the corner/cusp. Thus for such interfaces, the global error will depend on the width of the tubular neighborhood around the interface ϵ as stated in Theorem 4. We can also relate the errors to N; e.g., suppose that the error is $O(\epsilon^\tau)$: using $\epsilon = O(N^{-r})$, this error is equivalent to $O(N^{-r \cdot \tau})$. We point out that when ϵ is too small compared to h, the analytical theory that we develop in this paper no longer holds, as the problem becomes purely discrete. Such a scenario is analyzed in [6]. Finally, the optimal cost of constructing a distance function using the approaches reviewed in Section 2.1 is $O(N^{n-r})$, where r is the same as above.

Example 7. In this example, we compute integrals on the circle $x^2 + y^2 = r_0^2$, for $r_0 = 0.501$. We first study the accuracy of the extrapolative approach in computing the length of the circle, without using the distance function. The approximations are computed by the formula

$$S_N := \sum_{i,j} \epsilon^{-1} \delta_\epsilon(\epsilon^{-1}\phi_{i,j})|\nabla\phi_{i,j}|\, h^2,$$

where $\phi(x,y) = x^2 + y^2 - r_0^2$ and $\nabla\phi_{i,j}$ is evaluated with the exact formula of $\nabla\phi(ih, jh)$. In Table 1, we present our computations with radius $r_0 = 0.501$, and $\epsilon = 2h^{1/2}$ with $h = 2/N$, where N is the number of grid points along one coordinate direction. The analytical approximation error is $\mathcal{O}(\epsilon^2)$ for $\delta_\epsilon = \delta_{\infty,1}$, and $\mathcal{O}(\epsilon^3)$ for $\delta_{\infty,2}$, due to the number of vanishing moments that each kernel has. Provided that the corresponding quadrature error is negligible, with the scaling $\epsilon = 2h^{1/2}$, one should observe that, as $h \to 0$, the convergence rates for using $\delta_{\infty,1}$ is 1, and 1.5 for using $\delta_{\infty,2}$.

We point out that with the same ϵ at $N = 100$, if we used the signed distance function, $\phi(x,y) = \sqrt{x^2 + y^2} - r_0$ to the same circle, the relative error using $\delta_\epsilon = \delta_{\infty,1}$ would be $2.31890e{-}08$. This reflects the property of the integral $I[\tilde{f} \equiv 1, \phi](\eta)$, defined in (8), as a function of η.

Next, we study the accuracy of the extrapolative approach in integrating a Lipschitz continuous function defined on the same circle. In the computation, the level set function is the signed distance function $d(x,y) = \sqrt{x^2 + y^2} - r_0$, and the integrand f is defined by

$$f(x,y) = \min(|\theta - 0.3|, |\theta - 2\pi - 0.3|),\ 0 \le \theta = \arg(x,y) < 2\pi;$$

f is not differentiable along $\theta = 0.3$ and $\theta = \pi + 0.3$. In Figure 4 we present relative errors computed by the sum

$$S_N[f] := \epsilon^{-1} \sum_{i,j} f(ih, jh)\delta(\epsilon^{-1}\phi_{i,j})\, h^2,$$

with $\epsilon = 2\sqrt{h} = 2/\sqrt{N}$, and $\delta_\epsilon = \delta_{\infty,2}$. We observe the fast exponential convergence of the relative errors. On the one hand, we acknowledge that

$$I[f,\phi](\eta) = \int_{\Gamma_\eta} f dS,$$

is a degree one polynomial in η, even though f is only Lipschitz continuous. The chosen kernel $\delta_{\infty,2}$ has enough resolving power, and the analytical error of the approximation is zero. It is surprising, however, that the discretization errors converge so fast, even when the integrand is formally only Lipschitz continuous.

TABLE 1. Relative error in computing the circumference of a circle using a nondistance level set function.

	N=100	200	400	800	1600	3200
Rel. err. $\delta_{\infty,1}$	2.19034e-02	1.22417e-02	6.72509e-03	3.61084e-03	1.90462e-03	9.90744e-04
Order		0.8	0.9	0.9	0.9	0.9
Rel. err. $\delta_{\infty,2}$	2.99384e-03	1.53839e-03	6.34199e-04	2.55519e-04	9.96251e-05	3.78689e-05
Order		1.0	1.3	1.3	1.4	1.4
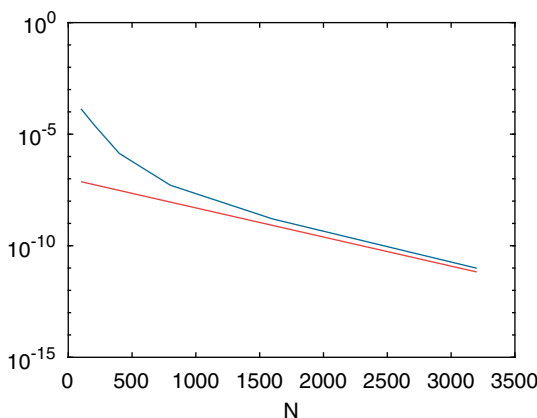
FIGURE 4. The blue curve reveals the relative errors computed by $S_N[f]$ for integrating a Lipschitz function on a circle. The red curve shows the graph of $0.997^N 10^{-7}$.

Example 8. In this example, we compute the length of the black curve shown in Figure 5, which has four cusps. The curve Γ_0 is defined by the four quarters of circles with radius $r_0 = 0.75$, centered respectively as $(r_0, 0), (-r_0, 0), (0, r_0)$ and $(0, -r_0)$.
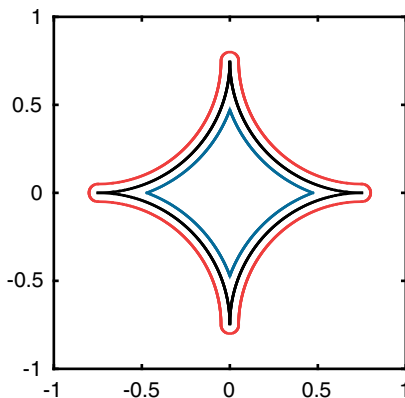

FIGURE 5. Cusp

The length is computed by the formula

$$S_N^+ := \sum_{i,j} \epsilon^{-1} \delta_{\infty,1}(\epsilon^{-1} d_{i,j}) \, h^2$$

using $\epsilon = 0.05$. The relative errors are tabulated in Table 2. The convergence in this example is actually exponential, namely the error decays like α^N, with $0 < \alpha < 1$. In this example, $\alpha \approx 0.9954$. Figure 6 shows the exponential convergence rate. Here $d_{i,j}$ denotes the value of the signed distance function to Γ_0 at the point (x_i, y_j). In the computations, the sign of the signed distance function to Γ_0 is designated to be negative inside the enclosed region. Note that the level sets of d in the region $\{d > 0\}$ are continuously differentiable. As the analysis in the above section shows, computations performed in $\{d < 0\}$ using

$$S_N^- := \sum_{i,j} \epsilon^{-1} \delta_{\infty,1}(-\epsilon^{-1} d_{i,j}) \, h^2,$$

will not yield accurate approximations due to the singularity of $I[\tilde{f} \equiv 1, \phi](\eta)$ near $\eta = 0^-$.

TABLE 2. Relative errors in computing the length of the black curve, containing four cusps, in Figure 5.

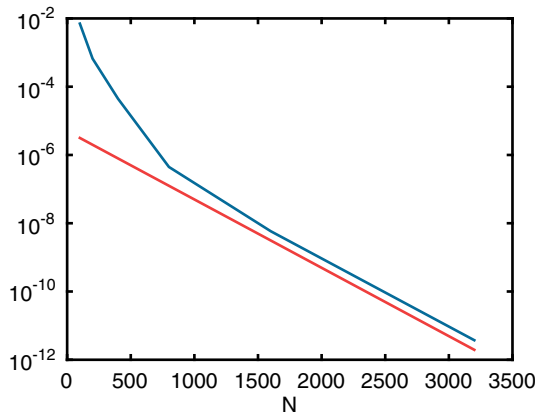| $w_{\infty,1}$	N=100	200	400	800	1600	3200
Rel.error S_N	7.04018e-3	6.63514e-4	4.43853e-5	4.45564e-7	5.84085e-9	3.74043e-12
Order		3.4	3.9	6.6	6.3	10.6

FIGURE 6. The blue curve reveals the relative errors computed by $S_N[f]$ for computing the length of the black curve with four cusps in Example 8. The red curve shows the graph of $5(0.9954)^N 10^{-6}$.

In Table 3, we present the numerical errors computed by $\tilde{S}_N^-$ to approximate the length of the interface which is 0.05 distance away from the black curve shown in Figure 5

$$\tilde{S}_N^- := \sum_{i,j,k} \epsilon^{-1} \delta_{\infty,1}(-\epsilon^{-1}(d_{i,j} + 0.05)) \, h^2.$$

TABLE 3. Relative errors in computing the length of the blue curve, containing four corners, in Figure 5. The theoretical convergence rate for this simulation is 2.0.

$w_{\infty,2}$	ϵ	N=100	200	400	800	1600	3200
Rel. error S_N	$3.4N^{-2/3}$	1.64925e-02	8.63529e-03	2.98334e-03	1.08381e-03	3.34617e-04	9.79520e-05
Order			0.9	1.5	1.5	1.7	1.8

Example 9. We compute the surface area of $\phi(x,y,z) := |x| + |y| + |z| = r_0$ (graphed in Figure 7) with $r_0 = 0.65$ by the following sum,

$$S_N := \sum_{i,j,k} \epsilon^{-1}\delta_{\infty,2}(\epsilon^{-1}\phi_{i,j,k})|\nabla\phi_{i,j,k}|h^3,$$

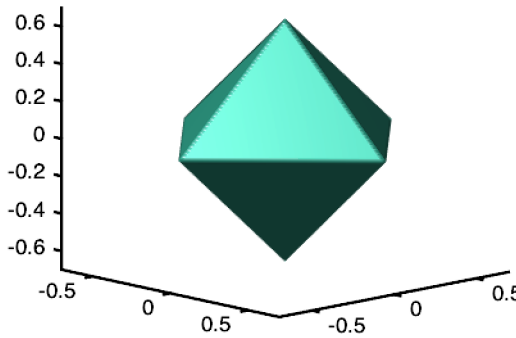where $|\nabla\phi_{i,j,k}| \equiv \sqrt{3}$.

FIGURE 7. Surface area of $|x| + |y| + |z| = r_0$ computed in Example 9.

The relative errors with $\epsilon = 0.1$ and a few values of $h = 1/N$ are presented in Table 4. The convergence rate in this simulation is also exponential and is illustrated in Figure 6. The point of this example is to demonstrate that the proposed approach is able to compute high order approximations of surface integrals, in the case where the surface and the embedding level set function are only piecewise smooth. This capability is not seen in other existing level set methods.

TABLE 4. Relative error in computing the surface area of an ℓ_1-ball.

	N=100	200	400	800
Rel. error	5.87232e-1	2.63126e-2	8.19894e-4	5.23091e-6
Order		4.5	5.0	7.3

Example 10. In this example, we compute the line integral of a function that has an integrable singularity at a corner of the interface. Let $\phi^{(1)}(x,y) := |x| + |y| - 1$, $\phi^{(2)}(x,y) = \operatorname{sgn}(\phi^{(1)}(x,y))\left(\phi^{(1)}(x,y)\right)^2$, where $\operatorname{sgn}(z)$ is the signum function.
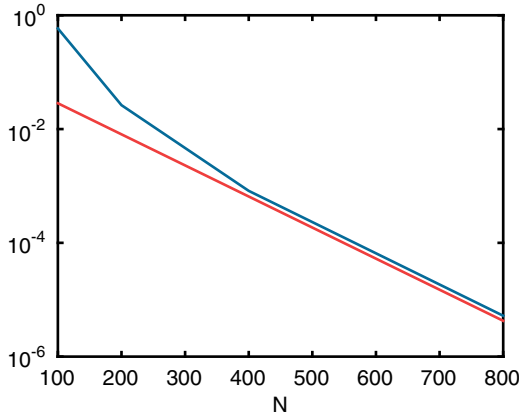
FIGURE 8. The blue curve reveals the relative errors computed by $S_N[f]$ for computing the surface area of the ℓ^1 ball described in Example 9. The red curve shows the graph of $0.9875^N 10^{-1}$.

Thus Γ_0 is the ℓ_1-ball. Analytically, the gradients of $\phi^{(1)}$ and $\phi^{(2)}$ exist almost everywhere. So in our computation, we globally define the gradients to be $|\nabla \phi_{i,j}^{(1)}| = \sqrt{2}$ and $|\nabla \phi_{i,j}^{(2)}| = \sqrt{8|\phi_{i,j}^{(2)}|}$. Let $f(r) = 1/\sqrt{r}$ for $r \neq 0$ and $f(0) = 10^9$. We define the interface $\Gamma_0 := \{\phi = 0\}$ and we approximate the integral

$$\int_{\Gamma_0} f(\sqrt{x^2 + (y-1)^2})dS(x,y)$$

by

$$S_N^{(\ell)} := \sum_{i,j} f(\sqrt{x_i^2 + (y_j - 1)^2})\epsilon^{-1}\delta_\epsilon(\epsilon^{-1}\phi_{i,j}^{(\ell)})|\nabla \phi_{i,j}^{(\ell)}|h^2,$$

where $\delta_\epsilon = \delta_{0.1,\infty,1}$. In Table 5, we present numerical errors of our computations, where ϵ is adjusted for each kernel so that the same number of points are used in the narrow bands $\{0.1\epsilon < |\phi_{i,j}^{(1)}| < \epsilon\}$ and $\{0.1\epsilon < |\phi_{i,j}^{(2)}| < \epsilon\}$.

This is an example that suggests the potential of the proposed extrapolative approach in computing integrands involving integrable singularities. For integration of singularities such as $1/\sqrt{x}$ in the interval $[0,1]$, one typically needs to require that the step size $h = h(x)$ decreases sufficiently fast as x tends to 0, otherwise, the resulting quadrature will have a significant drop in the order of accuracy. However, as Table 5 shows, the relative errors computed with $\phi^{(1)}$ decrease very slowly, but they are all under 1%; the relative errors computed with $\phi^{(2)}$ decrease steadily as the mesh refines.

There are three factors that determine the performance of the algorithm. The first one is the use of an extrapolative kernel which tends to zero as the value of the level set function goes to zero. Therefore, the singularity of the integrand is suppressed. Second, we observe that near $(0,1)$, the singularity of f, $|\nabla \phi^{(2)}(x,y)|$ is small, and the product does not have a singularity. See Figure 9 for the graph of $f |\nabla \phi^{(2)}|$. However, the derivative of $f |\nabla \phi^{(2)}|$ is unbounded at $(0,1)$, therefore, we
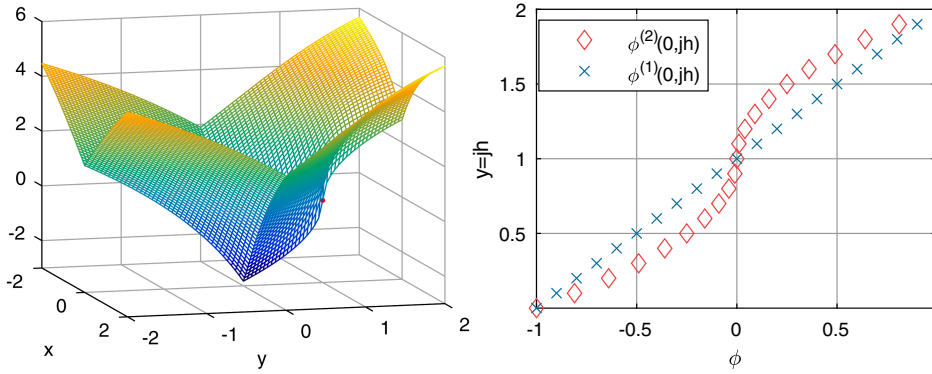
FIGURE 9.   Left: The graph of $f(x,y)|\nabla\phi^{(2)}(x,y)| :=$ $f(x,y)\sqrt{8\phi(2)(x,y)}$. The red dot indicates where the integrand is singular. Right: $\{\phi^{(1)}(0,jh) : j = 0,\pm1,\pm2,\ldots\}$ and $\{\phi^{(2)}(0,jh) : j = 0,\pm1,\pm2,\ldots\}$ have different spacings. The density of the latter increases as the absolute value of $|\phi^{(2)}(0,jh)|$ is closer to 0.

TABLE 5. Relative errors in the computation of a singular integral. The observed slow convergence resulting from using $\phi^{(1)}$ is expected, as the grid cannot resolve the singularity in $f|\nabla\phi^{(1)}|$. On the contrary, the quadrature with $\phi^{(2)}$ does better, at least ratewise, and the corresponding computation produces decreasing errors as N increases.

Ker=$w_{\delta,\infty,1}$	ϵ	N=200	400	800	1600	3200
Rel. err. $\phi^{(1)}$	$a_0 N^{-0.475}$	1.01552e-02	8.84065e-03	7.63649e-03	6.55206e-03	5.59749e-03
Order			0.2	0.2	0.2	0.2
Rel. err. $\phi^{(2)}$	$a_0^2 N^{-0.95}$	1.77161e-02	9.47018e-03	4.62084e-03	1.51821e-03	4.30993e-04
Order			0.9	1.0	1.6	1.8

expect that typical methods based on uniform grids will have deterioration in the accuracy and the convergence rate. However, the results reported in Table 5 are surprisingly better. Finally, the level set function $\phi^{(2)}$ is proportional to the squared distance to the interface Γ (the zero level set of $\phi^{(2)}$), and when discretized with a uniform grid, one has effectively an adaptive meshing with quadratic refinement in the step size in the direction normal to the interface. See Figure 9 for an illustration comparing the discretization resulting from $\phi^{(1)}(0,jh)$ and $\phi^{(2)}(0,jh)$.

Rigorous analysis of our approach to this type of singular integrals is the subject of another paper.

6. DISCUSSION

In this section, we compare this new approach with the original KTT approach constructed in [7] and discuss the potentials of the extrapolative approach for hypersurfaces with singularities. For smooth hypersurfaces, the original and the extrapolative approach both yield an exact result, namely the volume integral coincide exactly with the hypersurface integral one wishes to compute. However, exactness

is not obtained the same way. The original approach needs a Jacobian term in the integrand: this Jacobian corrects for the change in curvature incurred when one moves away from the hypersurface (namely the zero level set of the level set function). The extrapolative approach does not have a Jacobian but instead requires the approximation of the Dirac delta function to have at least $n-1$ vanishing moments, where n is the dimension. While the choice of the method is ultimately up to the practitioner, we believe it is easier to use the original approach on smooth hypersurfaces since (a) the Jacobian is easy to compute using the singular values of the Jacobian matrix of the closest point mapping (see [8]), and (b) there is no need to construct kernels with large numbers of vanishing moments, other than accuracy gain.

On the other hand, while the original approach suffers from low accuracy when used on hypersurfaces with singularities, the extrapolative approach is better suited for such cases. That said, we point out that for hypersurfaces with singularities, neither one of these two approaches will yield an integral formulation that coincides exactly with the hypersurface integral. However, the extrapolative approach is able to achieve good accuracy on hypersurfaces with corners, while the original approach does not perform well on any hypersurfaces with singularities. Unlike the original approach, the extrapolative one looks at a family of functionals in η, where η is the distance from a shifted level set and the hypersurface. In that case, if the singularity is a corner, the family of functionals will be a polynomial in η and thus, the accuracy will depend on the number of vanishing moments of the kernel. This approach is therefore capable of achieving high accuracy for computations of integrals over piecewise smooth hypersurfaces. For cusps, the family of functionals is not polynomial in η but a series with fractional powers in η. In that case, our analysis suggests that it is necessary to construct a different class of kernels with "fractional vanishing moments" in order to achieve high accuracy. Nevertheless, this extrapolative approach provides a stepping stone towards computing over hypersurfaces with singularities. In addition, we have shown a numerical simulation that suggests the potential of this technique for integrating functions with integrable singularities.

7. Conclusion

We described an extrapolative approach for integrating over hypersurfaces in the level set framework. This method is based on the classical integral formulation using an approximation of the Dirac delta function typically used with level sets. This analytical integral formulation is for most cases an approximation of the integral one wishes to compute. We show that for smooth interfaces, if the kernel approximating the Dirac delta function has enough vanishing moments, the integral formulation is actually equal to the hypersurface integral. In addition, unlike previous numerical integration schemes for level sets, we demonstrate that this method is capable of computing a line or surface integral with very high accuracy in the case where the hypersurface is only piecewise smooth (e.g., with corners). Finally, with an appropriate choice of kernel approximating the Dirac delta function, we can also compute integrals where the integrand has an integrable singularity. In particular, this work lays the foundation of a numerical scheme for computing general improper integrals.

References

[1] M. Burger, O.L. Elvetun, and M. Schlottbom, *Analysis of the diffuse domain method for second order elliptic boundary value problems*, Foundations of Computational Mathematics (2015), 1–48.

[2] C. Chen, C. Kublik, and R. Tsai, *An implicit boundary integral method for interfaces evolving by Mullins-Sekerka dynamics*, Submitted.

[3] C. Chen and R. Tsai, *Implicit boundary integral methods for the Helmholtz equation in exterior domains*, UCLA CAM Report 16-38.

[4] L.-T. Cheng and Y.-H. Tsai, *Redistancing by flow of time dependent eikonal equation*, J. Comput. Phys. **227** (2008), no. 8, 4002–4017, DOI 10.1016/j.jcp.2007.12.018. MR2403875

[5] J. Dolbow and I. Harari, *An efficient finite element method for embedded interface problems*, Internat. J. Numer. Methods Engrg. **78** (2009), no. 2, 229–252, DOI 10.1002/nme.2486. MR2510520

[6] B. Engquist, A.-K. Tornberg, and R. Tsai, *Discretization of Dirac delta functions in level set methods*, J. Comput. Phys. **207** (2005), no. 1, 28–51, DOI 10.1016/j.jcp.2004.09.018. MR2143581

[7] C. Kublik, N. M. Tanushev, and R. Tsai, *An implicit interface boundary integral method for Poisson's equation on arbitrary domains*, J. Comput. Phys. **247** (2013), 279–311, DOI 10.1016/j.jcp.2013.03.049. MR3066175

[8] C. Kublik and R. Tsai, *Integration over curves and surfaces defined by the closest point mapping*, Res. Math. Sci. **3** (2016), Paper No. 3, 17, DOI 10.1186/s40687-016-0053-1. MR3486053

[9] W. Lorensen and H. Cline, *Marching cubes: a high resolution 3d surface construction algorithm*, Computer Graphics **21** (1987).

[10] E. Maitre and F. Santosa, *Level set methods for optimization problems involving geometry and constraints. II. Optimization over a fixed surface*, J. Comput. Phys. **227** (2008), no. 22, 9596–9611, DOI 10.1016/j.jcp.2008.07.011. MR2467635

[11] B. Müller, F. Kummer, and M. Oberlack, *Highly accurate surface and volume integration on implicit domains by means of moment-fitting*, Internat. J. Numer. Methods Engrg. **96** (2013), no. 8, 512–528, DOI 10.1002/nme.4569. MR3130061

[12] S. Osher and R. Fedkiw, *Level Set Methods and Dynamic Implicit Surfaces*, Applied Mathematical Sciences, vol. 153, Springer-Verlag, New York, 2003. MR1939127

[13] S. J. Osher and F. Santosa, *Level set methods for optimization problems involving geometry and constraints. I. Frequencies of a two-density inhomogeneous drum*, J. Comput. Phys. **171** (2001), no. 1, 272–288, DOI 10.1006/jcph.2001.6789. MR1843648

[14] S. Osher and J. A. Sethian, *Fronts propagating with curvature-dependent speed: algorithms based on Hamilton-Jacobi formulations*, J. Comput. Phys. **79** (1988), no. 1, 12–49, DOI 10.1016/0021-9991(88)90002-2. MR965860

[15] G. Russo and P. Smereka, *A remark on computing distance functions*, J. Comput. Phys. **163** (2000), no. 1, 51–67, DOI 10.1006/jcph.2000.6553. MR1777721

[16] S. J. Ruuth and B. Merriman, *A simple embedding method for solving partial differential equations on surfaces*, J. Comput. Phys. **227** (2008), no. 3, 1943–1961, DOI 10.1016/j.jcp.2007.10.009. MR2450979

[17] R. I. Saye, *High-order quadrature methods for implicitly defined surfaces and volumes in hyperrectangles*, SIAM J. Sci. Comput. **37** (2015), no. 2, A993–A1019, DOI 10.1137/140966290. MR3338676

[18] P. Schwartz, D. Adalsteinsson, P. Collela, A. P. Arkin, and M. Onsum, *Numerical computation of diffusion on a surface*, Proc. Natl. Acad. Sci. USA **102** (2005), 11151–11156.

[19] J. A. Sethian, *A fast marching level set method for monotonically advancing fronts*, Proc. Nat. Acad. Sci. U.S.A. **93** (1996), no. 4, 1591–1595, DOI 10.1073/pnas.93.4.1591. MR1374010

[20] J. A. Sethian, *Level Set Methods and Fast Marching Methods*: *Evolving Interfaces in Computational Geometry, Fluid Mechanics, Computer Vision, and Materials Science*, 2nd ed., Cambridge Monographs on Applied and Computational Mathematics, vol. 3, Cambridge University Press, Cambridge, 1999. MR1700751

[21] P. Smereka, *The numerical approximation of a delta function with application to level set methods*, J. Comput. Phys. **211** (2006), no. 1, 77–90, DOI 10.1016/j.jcp.2005.05.005. MR2168871

[22] J. D. Towers, *Two methods for discretizing a delta function supported on a level set*, J. Comput. Phys. **220** (2007), no. 2, 915–931, DOI 10.1016/j.jcp.2006.05.037. MR2284331

[23] Y.-H. R. Tsai, L.-T. Cheng, S. Osher, and H.-K. Zhao, *Fast sweeping algorithms for a class of Hamilton-Jacobi equations*, SIAM J. Numer. Anal. **41** (2003), no. 2, 673–694, DOI 10.1137/S0036142901396533. MR2004194

[24] J. N. Tsitsiklis, *Efficient algorithms for globally optimal trajectories*, IEEE Trans. Automat. Control **40** (1995), no. 9, 1528–1538, DOI 10.1109/9.412624. MR1347833

[25] X. Wen, *High order numerical quadratures to one dimensional delta function integrals*, SIAM J. Sci. Comput. **30** (2008), no. 4, 1825–1846, DOI 10.1137/070682939. MR2407143

[26] X. Wen, *High order numerical methods to three dimensional delta function integrals in level set methods*, SIAM J. Sci. Comput. **32** (2010), no. 3, 1288–1309, DOI 10.1137/090758295. MR2652078

[27] X. Wen, *High order numerical methods to two dimensional delta function integrals in level set methods*, J. Comput. Phys. **228** (2009), no. 11, 4273–4290, DOI 10.1016/j.jcp.2009.03.004. MR2524518

[28] S. Zahedi and A.-K. Tornberg, *Delta function approximations in level set methods by distance function extension*, J. Comput. Phys. **229** (2010), no. 6, 2199–2219, DOI 10.1016/j.jcp.2009.11.030. MR2586244

Department of Mathematics, University of Dayton, 300 College Park, Dayton, Ohio 45469

E-mail address: `ckublik1@udayton.edu`

Department of Mathematics, KTH Royal Institute of Technology, SE-100 44 Stockholm, Sweden — and — Department of Mathematics and Institute for Computational Engineering and Sciences, University of Texas at Austin, 2515 Speedway, Austin, Texas 78712

E-mail address: `ytsai@ices.utexas.edu`